Elasto-plastic deformation within diamond reinforced metals for thermal management

M. Schöbel, P. Dobron, J. Bernardi, R. Wimpory, Kay A. Weidenmann

Angaben zur Veröffentlichung / Publication details:

Schöbel, M., P. Dobron, J. Bernardi, R. Wimpory, and Kay A. Weidenmann. 2016. "Elasto-plastic deformation within diamond reinforced metals for thermal management." *Diamond and Related Materials* 70: 52–58. https://doi.org/10.1016/j.diamond.2016.09.027.

Elasto-plastic deformation within diamond reinforced metals for thermal management

M. Schöbel [a,b,*], P. Dobron [c], J. Bernardi [d], R. Wimpory [e], K. Weidenmann [f]

[a] Forschungs-Neutronenquelle Heinz Maier-Leibnitz (FRM II), TU München, Lichtenbergstraße 1, 85747 Garching, Germany
[b] Lloyd's Register, EMEA, Business Area Energy, Opernring 1, 1010 Vienna, Austria
[c] Department of Physics of Materials, Faculty of Mathematics and Physics, Charles University in Prague, Ke Karlovu 3, CZ-121 16 Prague 2, Czech Republic
[d] Service Center for Electron Microscopy (USTEM), Technische Universität Wien, Wiedner Hauptstraße 8, 1040 Vienna, Austria
[e] Helmholtz Zentrum Berlin, Wannsee, Hahn Meitner Platz 1, 14109 Berlin, Germany
[f] Institute for Applied Materials, Karlsruhe Institute of Technology, Kaiserstraße 12, 76131 Karlsruhe, Germany

1. Introduction

In power electronic modules (insulated gate bipolar transistor units, IGBT), laptop processors and laser diodes (slab crystal housings), the increasing demand on thermal management requires appropriate heat sink materials [1,2]. Particle reinforced composites are promising candidates, combining the thermal properties of a highly conductive metal matrix with ceramic particles exhibiting low coefficients of thermal expansion (CTE) [3]. A high thermal conductivity (TC) is realized in SiC particle reinforced aluminum (Al-SiC), which are used to replace Cu heat sinks [4]. In such particle reinforced metals (PRM) the Al matrix combines its thermal properties of TC_{Al} ~ 240 W/mK and CTE_{Al} ~ 25 ppm/K with those of SiC with TC_{SiC} ~ 140 W/mK and CTE_{SiC} ~ 4 ppm/K resulting thermal properties of TC_{AlSiC} ~ 180 W/mK and CTE_{AlSiC} ~ 9 ppm/K for composites containing 70 vol.% bimodal SiC particles [5,6]. These properties provide sufficient heat dissipation through the metal matrix and concomitantly reduce the thermal mismatch stresses with the adjacent ceramic substrate, thereby increasing the long term stability of the system loaded with thermal cycles [3].

Metal matrices reinforced with up to 60 vol.% monomodal diamond particles are developed to replace Al-SiC as heat sink material [7]. Carbon diamond (CD) offers the highest thermal conductivity TC_{CD} > 2000 W/mK combined with almost no thermal expansion of CTE_{CD} ~ 1 ppm/K [8,9] achieving thermal properties of AlCD composites of TC_{AlCD} ~ 500 W/mK and CTE_{AlCD} ~ 6 ppm/K [10–13], both improved with respect to Al-SiC [14]. The best performance has been achieved by a silver matrix reinforced by CD particles [13,15,16] exhibiting TC_{AgCD} > 800 W/mK [7,13]. Such PRM are developed for satellite laser optics, where the economic limitations are less restrictive.

The major problem with diamond particles is their poor wettability by liquid metals during infiltration and the resulting low interface bonding strength [9,17,18]. Liquid metal infiltration of densely packed particle preforms comprising up to 60 vol.% CD-particles may produce infiltration voids, which may be harmful to the structural stability as well as to the thermal properties of the PRM [19–21]. However, the shrinking of the solidifying metal matrix in between the particles causes

* Corresponding author at: Lloyd's Register, EMEA, Business Area Energy, Opernring 1, 1010 Vienna, Austria.
E-mail address: michael.schoebel@lr.org (M. Schöbel).

mandatorily initial voids, which will grow during cooling owing to the CTE mismatch of the composite's components [22]. Such shrinkage voids in a composite with sufficient particle-matrix interface bonding strength can be useful to reduce thermal mismatch stresses by elasto-plastic matrix deformation during temperature changes [23]. Therefore, infiltration quality and interface bonding strength are the key issues of CD reinforced MMC to achieve high thermal conductivity and low thermal expansion for long term operation conditions under cycling thermal loads [7,16,25,27].

The high CTE mismatch between matrix and reinforcement (ΔCTE ~ 24 ppm/K in AlCD, ΔCTE ~ 18 ppm/K in AgCD) will lead to high micro stresses and severe matrix deformation near the particle interfaces [26]. Interface delamination initiates thermal fatigue damage in such heat sink materials [24,25]. The interface bonding strength [17] and matrix deformability [27] is the key to successful material selection for demanding thermal management with sufficient long term stability.

The AlCD composites benefit from the low cost of aluminum as matrix material, its castability and interface reactivity [8,11]. In order to support carbide formation to increase the bonding strength of the plane crystallographic diamond surfaces, the particle filled preforms are heat treated prior to the liquid metal infiltration. In case of the AgCD composites a high interface reactivity and bonding strength can be achieved by alloying the matrix with Si, as shown in previous investigations [15,16].

In particle reinforced composites with a stiff ceramic reinforcement embedded in a ductile matrix metal, high micro stress gradients lead to partial plastification of the ductile phase [27]. The stress gradients by diamond reinforcements should be favorably accommodated by elasto-plastic matrix deformation [23] counteracting damage mechanisms such as cracking or delamination. Interconnectivity of a network-like reinforcement structure [26] may provoke crack formation in this network [27] under mechanical loads. In contrast to isolated particles embedded in a ductile matrix phase, which is able to deform and consequently, high interfacial micro stress gradients relax [14]. In the following, elasto-plastic deformation in Al/CD/60p composites in two different conditions is compared with AgSi11/CD/60p under externally applied stress. The deformation behavior of a carbon diamond particle reinforced ductile matrix is compared with that of a relatively brittle matrix by in-situ non-destructive testing techniques.

2. Experiment

2.1. Materials description

Three different diamond particle reinforced composites were investigated (Table 1). All composites were produced by gas pressure assisted liquid metal infiltration [28] at the Laboratory for Mechanical Metallurgy of EPF Lausanne in Switzerland.

The synthetic diamond powder was purchased from Luoyang High-Tech Qiming Superhard Materials Co. Ltd., China. A monomodal diamond powder of the grit mesh size 500/600 (average particle diameter of about 22 μm) was used to produce densely packed preforms of particle content of 60 vol.%. The preforms for the Al/CD/60p composites were heated to the infiltration temperature of 800 °C. Furthermore, the temperature was kept for 3 h or 10 h in vacuum to stimulate graphite formation at the diamond particle surfaces. Both conditions were infiltrated by pressing the liquid aluminum with 15 bar into the mold. The preforms are completely infiltrated after 3 min and the pressure was subsequently released during cooling. Although the thermal conductivity of the interfaces will be reduced by carbide formation on the diamond particles, long term integrity of the composites (i.e. reduced interface delamination) is improved. Therefore great emphasis is given to investigate the influence of carbides on interface bonding strength.

The AgSi11/CD/60p composites were produced by the same method with the preform initially heated to the infiltration temperature of 1050 °C held there for 30 min and then pressure infiltrated by the liquid alloy at 22.5 bar pressure. Again, the preform is supposed to be completely infiltrated after 3 min and the pressure subsequently released after solidification, while the mold is cooled. The materials were cast in the shape of tensile test specimens as used for previously performed mechanical tests [16]. The dimensions of the tensile test specimens' gauges are 25 × 6 × 2.5 mm. Two specimens for each composite type were used for the following neutron diffraction and acoustic emission measurements.

2.2. Neutron diffraction

Angle dispersive neutron diffraction (ND) was performed at E3 strain scanner at HZB Wannsee, Germany [29] using a monochromatic neutron beam with $\lambda = 1.486$ Å and flux ~5×10^6 n cm^{-2} s^{-1} through the sample. A 50 kN tensile test equipment was mounted on the x,y,z-table for the in-situ strain measurements [30]. The same sample dimensions have been used for previous investigations [16]. A primary aperture of 6 × 6 mm^2 and a secondary of 6 mm width ensured a complete flooding of the test specimens' cross section of 6 × 2.5 mm^2 within the neutron beam. The 2D^{3}He position sensitive detector (PSD) unit with 256 × 256 capillaries with a pixel size of 1.38 × 1.38 mm^2 was set to $2\theta = 42°$ for diamond (111) and $2\theta = 72°$ for diamond (220) for serial acquisition of the two most representative diamond lattice planes (according to CEN ISO/TS 21432:2005). The Ag (311) peak from AgSi11/CD/60p could be acquired additionally, due to the smaller grain size of the AgSi11alloy compared to the pure Al metal matrix, which could not be recorded.

The external tensile force was controlled by a calibrated load cell and stepwise increased (with 200 N/step for Al/CD/60p 10 h ht, 300 N/step for Al/CD/60p 3 h ht, 400 N/step for AgSi11/CD/60p and with 50 N/s load rate) in between the strain scans during tensile testing, starting from the initially unloaded condition. 5 min acquisition time was set to scan the CD (111) and CD (220) peak intensity (additionally, Ag (311) of AlSi11/CD/60p). The micro strains were evaluated in relation to the unloaded condition [27], neglecting the initial microstress state from casting (cooling after infiltration).

2.3. Acoustic emission

The acoustic emission (AE) was measured during tensile test experiments carried out like for neutron diffraction. The computer controlled DAKEL-IPL-4 AE data-streaming system was used for a continuous storage of emitted signals with 2 MHz sampling frequency. A miniaturized MST8S piezoelectric transducer (diameter of 3 mm, almost point AE detection, a frequency band from 100 to 600 kHz, sensitivity 55 dB at 1 V_{eff}) was attached to the specimens on the 6 mm wide side of their rectangular cross section. A good acoustic contact was ensured by using silicon grease and a small preloaded spring clamp. A preamplifier with a gain of 35 dB was used to reduce the AE noise-to-signal-ratio. The 12-

Table 1
Composition of diamond reinforced composites as used for the investigations.

Composite	Matrix 40 vol.%	Diamond 60 vol.%	Condition
Al/CD/60p 3 h ht	Al 99.99%	Ø ~ 22 μm	Particle preform heat treated for 3 h at 800 °C prior to infiltration
Al/CD/60p 10 h ht	Al 99.99%	Ø ~ 22 μm	Particle preform heat treated for 10 h at 800 °C prior to infiltration
AgSi11/CD/60p	Ag 89 at.%, Si 11 at.%	Ø ~ 22 μm	No additional particle heat treatment

bit A/D converter had a full scale of ±2 V. The acquired AE data were analysed by the DAKEL-UI software using a threshold-level detection with the threshold set to1.5 mV. The AE count rate (the count number per time unit at a given threshold voltage level) was evaluated according to ASTM E750-04.

2.4. Scanning electron microscopy

The microstructure of the fracture surfaces was investigated by scanning electron microscopy (SEM) with a FEI Quanta 250 FEG field emission gun operated at 15 kV. A standard Everhart Thornley detector (ETD) was used for secondary electron images (SE). Back scattered electron images were obtained by a concentric backscattered detector (CBS). The chemical composition of individual phases was identified by energy dispersive X-ray analysis using an EDAX detection system.

3. Results

The fracture surfaces of the broken tensile test specimens of the Al/CD/60p composite after 3 h heat treatment and that after 10 h treatment are compared in Figs. 1 and 2.

The monomodal diamond particles are well bonded to the plastically deformed Al-matrix after 3 h and 10 h heat treatment. The particle-matrix interfaces show good bonding with no interface delamination for both conditions in Figs. 1b and 2b. The plastically deformed matrix metal exhibits dimples near the particle-matrix interfaces with more particle fragmentations in the 10 h heat treated condition compared to the 3 h heat treated condition.

In AgSi11/CD/60p the fracture surface shows particle shaped imprints in the matrix metal, indicating brittle interface fracture in Fig. 3.

The α-Ag can be distinguished from Si particles in between the diamond particles in Fig. 3b. Good bonding quality can be observed by residual AgSi11 matrix on the plane CD surfaces. Partially fragmented particles are well embedded in the eutectic matrix metal with few indications of ductile matrix deformation.

Fig. 4 shows the strain evolution of the tensile test on Al/CD/60p after 10 h heat treatment (Table 1). The macroscopic stress strain can be compared to microscopic lattice strains in CD (111) and CD (220)

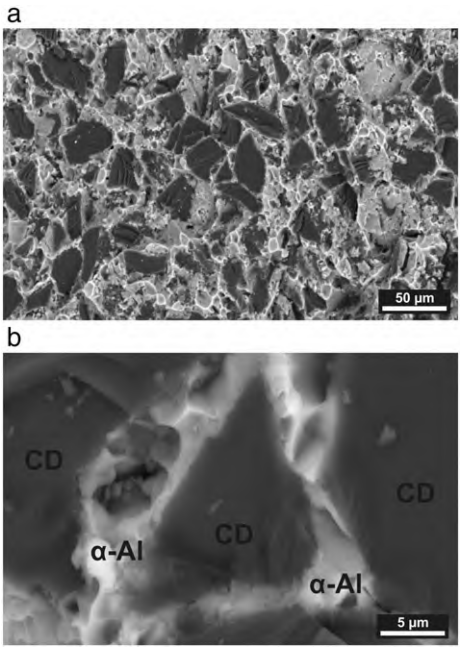

Fig. 1. SEM (BSE) image of a fracture surface of Al/CD/60p after 3 h heat treatment (Table 1); (a) densely packed diamond particles (dark) well embedded in Al-matrix (bright); (b) ductile matrix dimples and fractured well bonded particles after 3 h of heat treatment.

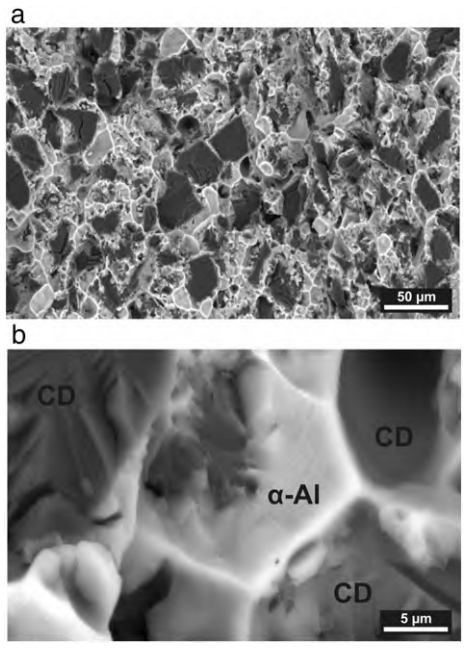

Fig. 2. SEM (BSE) image of a fracture surface of Al/CD/60p after 10 h heat treatment (Table 1); (a) densely packed diamond particles with surface fracture indications (dark) appear well embedded in ductile deformed Al matrix (bright); (b) ductile matrix dimples and fractured particles without indication of delamination.

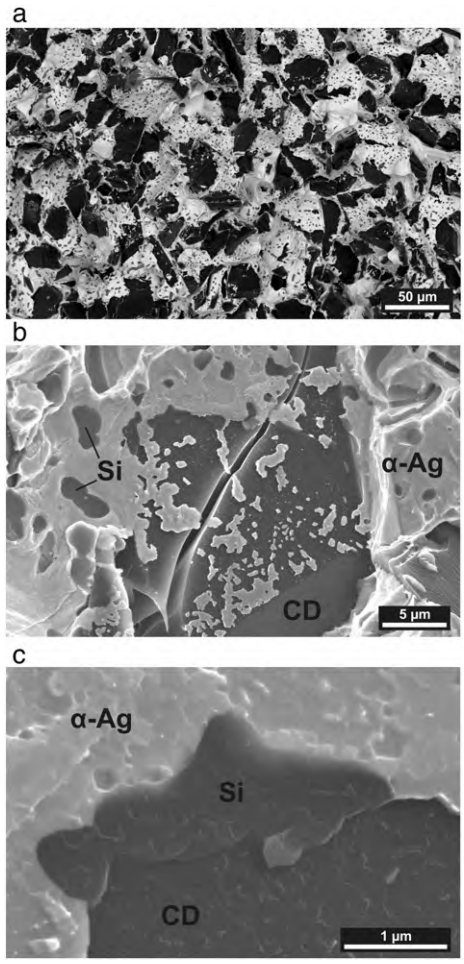

Fig. 3. SEM image of a fracture surface of AgSi11/CD/60p; (a) Diamond particles embedded in AgSi11 eutectic; (b) Si particles of the eutectic appear in between large diamond particles, one of which is cracked, (c) with Si bonded to the CD particle interfaces.

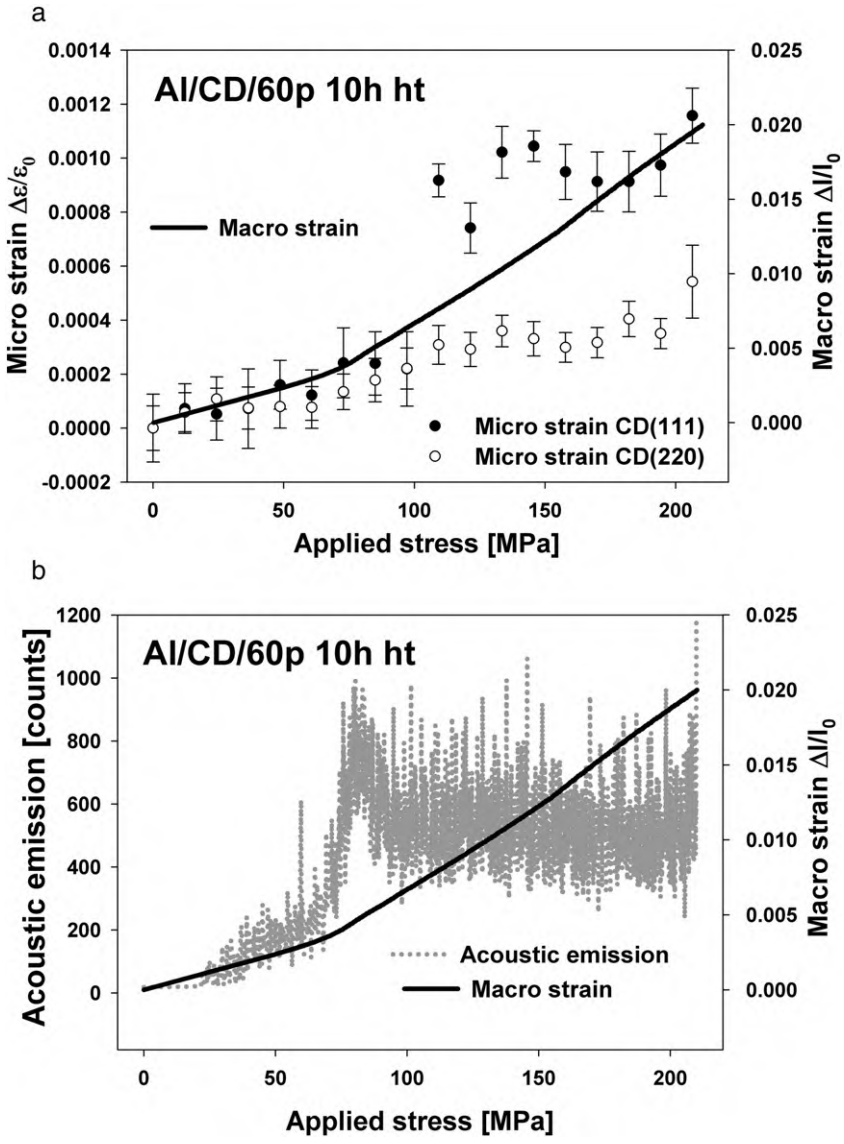

Fig. 4. Tensile test on Al/CD/60p after 10 h heat treatment (Table 1); (a) Macro strain compared to micro strain in diamond (111) and diamond (220); (b) macro strain compared to acoustic emission.

revealed by neutron diffraction (Fig. 4a). An elastic behavior can be initially observed until 70 MPa external loading is reached. Above 70 MPa the slope in the macroscopic strain increases, indicating the beginning of plastic matrix deformation. At 100 MPa, a significant jump of micro strain level is induced in CD (111). Above 100 MPa, where CD (220) linearly increases, the comparable high CD (111) strain level slightly increases until 150 MPa and remains saturated until fracture at 210 MPa. The acoustic emission measurement (Fig. 4b) identifies the same "silent" elastic region until 70 MPa, congruent to the constant slope of the macroscopic strain. The AE count rate exhibits a peak around 80 MPa which is related to the macroscopic yield strength. The level of the AE intensity remains roughly constant from 100 MPa onwards until fracture at 210 MPa. The macro and micro strains in Al/CD/60p after 3 h heat treatment (Table 1) are compared in Fig. 5.

In Al/CD/60p after 3 h heat treatment an initial elastic region until 70 MPa can be distinguished from an elasto-plastic regime above 70 MPa followed by a small strain increase in CD (111). However, the micro strain level is significantly lower than in the 10 h heat treated composite and fracture occurs already at 170 MPa. The low AE activity corresponds to small plastic deformation, i.e. load transfer from particles into the ductile matrix metal. Micro and macro strains in AgSi11/CD/60p (Fig. 6) show a similar behavior even in the Ag matrix (Fig. 6a).

The parallel strain evolution indicates elastic deformation of the diamonds while the matrix deforms plastically as well. The AE count rate increases as well continuously with increasing deformation of the Ag matrix until fracture at 170 MPa (Fig. 6b).

4. Discussion

In diamond reinforced aluminum composites Al/CD/60p the soft matrix metal becomes elasto-plastically deformed in between stiff diamond particles, when an external load is applied. The characteristic AE peak at the onset of plastic deformation, typically observed in metals [31], can be explained by a massive dislocation multiplication in the Al matrix. The subsequent decrease in the AE count rate can be assumed to be a consequence of an increasing number of sessile dislocations reducing the free path of moving dislocations. Based on this AE behavior, the bonding strength is higher than the matrix yield strength. The roughly constant AE activity from 100 MPa until fracture indicates the activation of different deformation and crack mechanisms. The deformation mechanisms in such composites allow accommodation of high micro stress in the matrix without significant interface damage. Heat treatment induced carbide formation at the interfaces increases the bonding strength [9], as proven by higher load transfer from the ductile

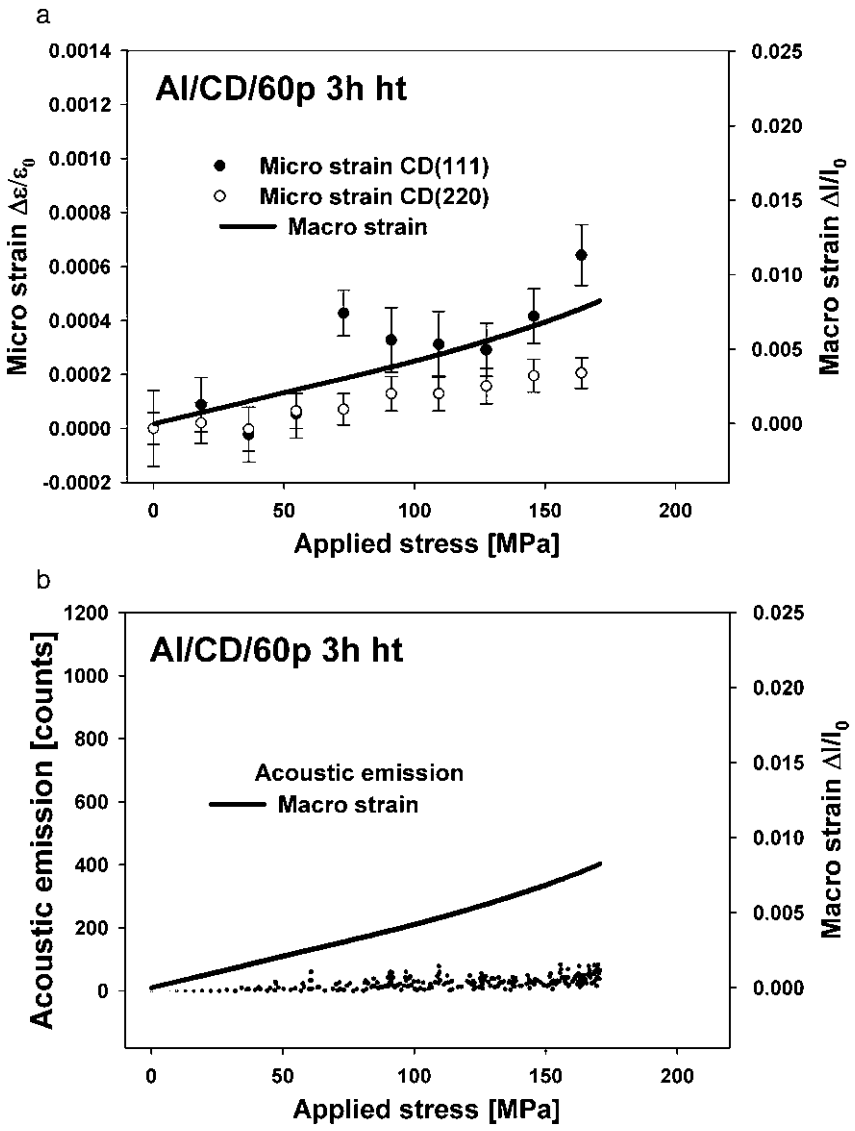

Fig. 5. Tensile test on Al/CD/60p after 3 h heat treatment (Table 1); (a) Macro strain compared to micro strain in diamond (111) and diamond (220); (b) Macro strain compared to acoustic emission.

matrix metal into the stiff diamond particles and by increased yield strength of samples after 10 h heat treatment compared to those heat treated for 3 h. A system of isolated particles was identified in Al/CD/60p, according to [26], which become heterogeneously deformed (elastic particle- and elasto-plastic matrix-deformation, depending on bonding strength) as soon as an external mechanical load is applied. A similar occurrence is observed in heterogeneous light alloys [27]. Therefore, a partial plastification of matrix regions close to the interface with particles occurs, if the external load passes 70 MPa. Elasto-plastic deformation of the matrix occurs above 70 MPa, proven by AE and ND. The load is heterogeneously transferred from the matrix metal into the stiff ceramic particles due to anisotropic elastic modulus and interface bonding strength. The observed heterogeneity in strain increase between two lattice planes of the diamonds indicates a difference in particle interface reactivity in terms of carbide formation after heat treatment [11]. If interface bonding is strong, the micro structure will suffer high micro stresses induced by external stresses which are accommodated by local matrix plastification in between high volume fractions of stiff diamond particles.

Deformation in diamond reinforced silver composites AgSi11/CD/60p remains elastically even above 100 MPa. External load transfer is stress controlled between diamond particles and the AgSi11 matrix. The diamond strain evolution appears homogeneously in different lattice planes, CD (111) and CD (220) with deviations caused by $E_{CD\{h,k,l\}}$ anisotropy and interface reactivity effects. The fracture surface indicates well bonded particles interconnected by the Si phase of the eutectic matrix. The same interconnected reinforcement architecture could be observed in AlSi7 matrix PRM from previous work [23,26]. The lower ductility of the matrix alloy provokes crack initiation giving rise to brittle fracture at the particle-matrix interfaces. The continuous increase in the AE count rate supports this scenario because initiation and propagation of cracks are excellent AE sources.

The consequence is lower fracture strength of the AgSi11/CD/60p compared to that of Al/CD/60p after 10 h heat treatment with improved interface strength by carbide formation.

5. Conclusions

In diamond reinforced aluminum composites heat treatments of the particle preform improves bonding strength above the yield strength of the pure Al matrix. The ductile metal matrix is able to accommodate high stress gradients by locally variable elasto-plastic deformation, particularly near the interfaces between the stiff diamond particles. The ductile aluminum matrix starts to flow above the elastic region and

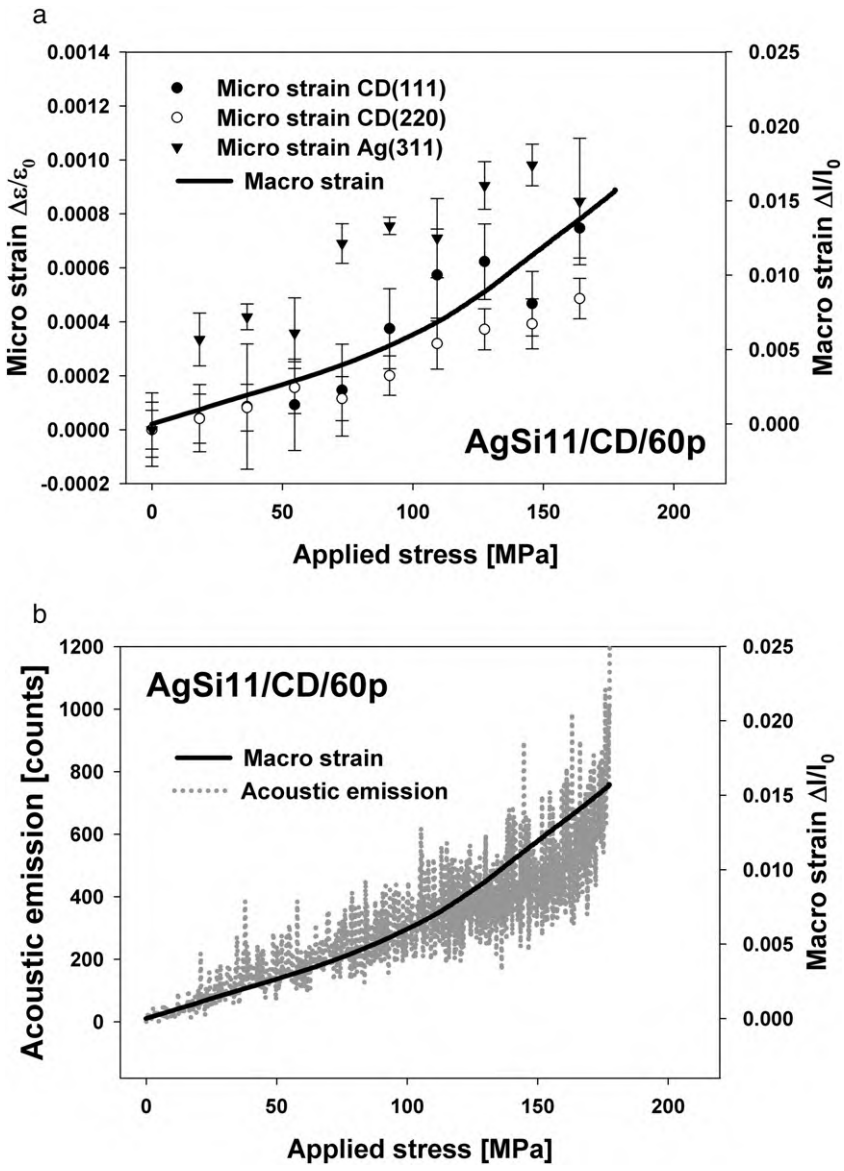

Fig. 6. Tensile test on AgSi11/CD/60p; (a) Macro strain compared to micro strain in diamond (111), diamond (220) and Ag (311); (b) Macro strain compared to acoustic emission.

deforms plastically until fracture, indicating an overall stiff but partial ductile deformation behavior of that AlCD composites. In the 10 h heat treated condition the fracture strain and elasto-plastic deformability (indicated by ND and AE) appear higher than after 3 h heat treatment. Increasing heat treatment time supports carbide formation at the particle-matrix interface, which significantly improves their bonding strength.

In AgSi11/CD/60p composites an eutectic matrix of α-Ag and Si phase is formed. Although the particle-matrix bonding appears strong, brittle fracture occurs before the composite like eutectic Ag-Si matrix shows ductile deformation. The result is low accommodation of stress gradients, leading to interfacial crack initiation and fracture. The eutectic matrix, consisting of an interconnected *Si*-diamond network structure, reduces elasto-plastic deformability of the AgSi11/CD/60p composite.

Micro stress concentrations at the interfaces in metal matrix composites may lead to crack initiation and failure under mechanical loading, particularly if the matrix forms brittle interfaces without exploiting the intrinsic mechanical capabilities of the different phases (like in the eutectic matrices). Therefore a ductile matrix with high particle-matrix bonding strength is preferred to accommodate high interface shear stresses.

Acknowledgements

The author M. Schöbel gratefully thanks H. Peter Degischer and Alun Rhys-Williams for support and proof-reading the manuscript.

References

[1] C. Zweben, Electronic packaging materials, Adv. Mater. Process. 163 (2005) 33–37.
[2] K. Yoshida, H. Morigami, Thermal properties of diamond/copper composite material, Microelectron. Reliab. 44 (2004) 303–308.
[3] C. Zweben, Metal-matrix composites for electronic packaging, J. Metal. 44 (1992) 15–23.
[4] G. Lefranc, H.P. Degischer, H.K. Sommer, G. Mitic, T. Massard, Al-SiC improves Reliability of IGBT Power ModulesICCM12, Paris, 1999.
[5] A. Joseph, I. King, Materials Handbook for Hybrid Microelectronics. Norwood, USA, 1988.
[6] A. Mortensen, Melt Infiltration of Metal Matrix Composites, in: A. Kelly, C. Zweben (Eds.), Comprehensive Composite Materials, vol. 3, Pergamon Press, Oxford 2000, pp. 541–547.
[7] K. Watari, L.S. Subash, High thermal conductivity materials, MRS Bull. 26 (2001) 440–441.
[8] M. Battabyal, O. Beffort, S. Kleiner, S. Vaucher, L. Rohr, Heat transport across the metal–diamond interface, Diam. Relat. Mater. 17 (2008) 1438–1442.

[9] S. Kleiner, F.A. Khalid, P.W. Ruch, S. Meier, O. Beffort, Effect of diamond crystallographic orientation on dissolution and carbide formation in contact with liquid aluminium, Sci. Mater. 55 (2008) 291.
[10] J.-M. Molina, M. Rheme, J. Carron, L. Weber, Thermal conductivity of aluminum matrix composites reinforced with mixtures of diamond and SiC particles, Scr. Mater. 58 (2008) 393–396.
[11] O. Beffort, F.A. Khalid, L. Weber, P. Ruch, U.E. Klotz, S. Meier, S. Kleiner, Interface formation in infiltrated Al(Si)/dimaond composites, Diam. Rel. Mater. 15 (2006) 1250–1260.
[12] L. Weber, R. Tavangar, On the influence of active element content on the thermal conductivity and thermal expansion of Cu–X (X = Cr, B) diamond composites, Scr. Mater. 57 (2007) 988–991.
[13] R. Tavangar, J.M. Molina, L. Weber, Assessing predictive schemes for thermal conductivity against diamond-reinforced silver matrix composites at intermediate phase contrast, Scr. Mater. 56 (2007) 357–360.
[14] X.-h. Qu, L. Zhang, W. M, S.-b. Ren, Review of metal matrix composites with high thermal conductivity for thermal management applications, Mater. Int. 21 (2011) 189–197.
[15] K.A. Weidenmann, R. Tavangar, L. Weber, Rigidity of diamond reinforced metals featuring high particle contents, Comp. Sci. Tech. 69 (2009) 1660–1666.
[16] K.A. Weidenmann, R. Tavangar, L. Weber, Mechanical behaviour of diamond reinforced metals, Mater. Sci. Engin. A 523 (2009) 226–234.
[17] S.W. Webb, Diamond retention in sintered cobalt bonds for stone cutting and drilling, Diam. Relat. Mater. 8 (1999) 2043–2052.
[18] C. Monachon, L. Weber, C. Dames, Thermal Boundary Conductance: A Materials Science Perspective, Annu. Rev. Mater. Res. 46 (2016) c. 8.1-8.31.
[19] P.W. Ruch, O. Beffort, S. Kleiner, L. Weber, P.J. Uggowitzer, Selective interfacial bonding in Al(Si)–diamond composites and its effect on thermal conductivity, Comp. Sci. Tech. 66 (2006) 2677–2685.
[20] I.E. Monje, E. Louis, J.M. Molina, On critical aspects of infiltrated Al/diamond composites for thermal management: diamond quality versus processing conditions, Comp. Part A 67 (2014) 70–76.
[21] I.E. Monje, E. Louis, J.M. Molina, Optimizing thermal conductivity in gas-pressure infiltrated aluminum/diamond composites by precise processing control, Comp. Part A 48 (2013) 9–14.
[22] M. Schöbel, G. Fiedler, D. Tolnai, S. Vaucher, G. Requena, H.P. Degischer, Void formation in metal matrix composites by solidification and shrinkage of an AlSi7 matrix between densely packed particles, Compos. Part A 66 (2014) 103–108.
[23] M. Schöbel, W. Altendorfer, H.P. Degischer, S. Vaucher, T. Buslaps, M. Di Micheli, M. Hofmann, Internal stresses and voids in SiC particle reinforced aluminum composites for heat sink applications, Comp. Sci. Tech. 71 (5) (2011) 724–733.
[24] M. Kouzeli, L. Weber, C. San Marchi, A. Mortensen, Influence of damage on the tensile behaviour of pure aluminium reinforced with ≥40 vol. pct alumina particles, Acta Mater. 49 (2001) 497–505.
[25] P.B. Pragnell, T. Downes, P.J. Withers, W.M. Stobbs, The deformation of discontinuously reinforced MMCs, Acta Metall. Mater. 42 (1994) 3437–3442.
[26] M. Schöbel, H.P. Degischer, S. Vaucher, M. Hofmann, P. Cloetens, Reinforcement architectures and thermal fatigue in diamond particle-reinforced aluminum, Acta Mater. 58 (19) (2010) 6421–6430.
[27] M. Schöbel, G. Baumgartner, M. Hofmann, J. Bernardi, Microstresses and crack formation in AlSi7MgCu and AlSi17Cu4 alloys for engine components, Acta Mater. 81 (2014) 401–408.
[28] O. Beffort, S. Vaucher, F.A. Khalid, On the thermal and chemical stability of diamond during processing of Al/diamond composites by liquid metal infiltration (squeeze casting), Diam. Relat. Mater. 13 (2004) 1834–1843.
[29] R.C. Wimpory, P. Mikula, J. Saroun, T. Poeste, J. Li, M. Hofmann, R. Schneider, Efficiency boost of the materials science diffractometer E3 at BENSC: one order of magnitude due to a horizontally and vertically focusing monochromator, Neutron News 19 (2008) 16–19.
[30] M. Hoelzel, W.M. Gan, M. Hofmann, C. Randau, G. Seidl, P. Jüttner, W.W. Schmahl, Rotatable multifunctional load frames for neutron diffractometers at FRM II—design, specifications and applications, Nuc. Inst. A 711 (2013) 101–105.
[31] P. Dobron, J. Bohlen, F. Chmelik, P. Lukac, D. Letzig, K.U. Kainer, Acoustic emission during stress relaxation of pure magnesium and AZ magnesium alloys, Mater. Sci. Engi.: A 462 (2007) 307–310.